Pregnancy Hypertension 17 (2019) 216–225

Contents lists available at ScienceDirect

Pregnancy Hypertension

journal homepage: www.elsevier.com/locate/preghy

Circular RNA expression profiling identifies hsa_circ_0011460 as a novel molecule in severe preeclampsia

Na Deng[a,1], Di Lei[a,1], Jinfa Huang[a,1], Zhuanhong Yang[b], Cuifang Fan[a,*], Suqing Wang[b,*]

[a] Department of Obstetrics and Gynecology, Renmin Hospital of Wuhan University, Wuhan 430060, China
[b] Department of Nutrition and Food Hygiene, School of Health Science, Wuhan University, 185, Donghu Rd, Wuhan, Hubei 430071, China

ARTICLE INFO

Keywords:
Preeclampsia
Circular RNA
RNA-Seq
Placenta

ABSTRACT

Objectives: To identify circRNA expression profiles in the placentae of severe preeclampsia (SPE) and normal pregnant (NP) women.

Methods: Placental samples were collected from six paired SPE and NP women. CircRNA expression profiles were identified by RNA-Seq and validated in another 30 SPE and NP samples by qRT-PCR. Several bioinformatic tools were utilised to analyse the potential function of differentially expressed circRNAs (DE-circRNAs) and to predict target microRNAs (miRNAs) and proteins. Furthermore, immunohistochemistry, Western blotting and RNA binding protein immunoprecipitation (RIP) were conducted to confirm the interaction between the circRNA and protein.

Results: In total, 18,631 circRNAs were detected. Among them, 180 circRNAs were differentially expressed, including 94 upregulated and 86 downregulated circRNAs. Seven DE-circRNAs were selected for validation, and the results of six circRNAs (hsa_circ_0007611, hsa_circ_0011460, hsa_circ_0002888, and hsa_circ_0007445, hsa_circ_0017068, hsa_circ_0012737) were consistent with the sequencing results. Bioinformatics analyses of DE-circRNAs revealed that most of them are involved in vasodilation, regulation of blood vessel size, protein transport and localization, and pathways in cancer. In addition to the mRNA expression profile, it was interesting to find that the hsa_circ_0011460 target gene solute carrier organic anion transporter family member 2A1 (SLCO2A1, PGT) was also significantly increased in SPE placentae. Immunohistochemistry, Western blotting and qRT-PCR validated the expression and distribution of PGT. Finally, RIP of HTR-8/SVneo cells confirmed that hsa_circ_0011460 targets PGT directly.

Conclusions: A total of 180 DE-circRNAs were detected. One crucial circRNA, hsa_circ_0011460, was shown to interact directly with its host gene PGT. These findings indicated that hsa_circ_0011460 may serve as a potential therapeutic target for patients with SPE.

1. Introduction

Preeclampsia (PE) affects 3%–5% of human pregnancies and keeps the leading cause of perinatal morbidity and mortality worldwide, especially in low-income and middle-income countries [1]. The aetiology and pathogenesis of PE remains unclear. Timely termination of delivery is the only effective treatment for PE, while women with PE are still at a greater risk of developing cardiovascular complications later in life.

CircRNAs, a class of noncoding RNA, are characterized by a covalent bond linking the 3′ and 5′ ends generated by backsplicing. These molecules were often considered to be aberrant splicing by-products with little functional potential for tens of years [2]. In recent years, the rapid advancement of high-throughput RNA sequencing technology has catalysed the in-depth study of circRNAs, which have been implicated in the physiological progress and pathogenesis of various diseases and conditions, such as neural development, human epithelial-mesenchymal transition (EMT) progress and cancer development [3,4]. At the molecular level, these molecules regulate gene expression by titrating miRNAs, sequestering proteins, modulating RNA polymerase II transcription, and interfering with pre-mRNA processing [5]. Two of the best-known circRNAs, ciRS-7/CDR1as and Sry circRNA, have been characterized as miRNA sponges [4,6]. However, it should be noted that the majority of circRNAs in mammals are expressed at low levels

* Corresponding authors at: Department of Obstetrics and Gynecology, Renmin Hospital of Wuhan University, 238 Jiefang Road, Wuhan, Hubei 430060, China (C. Fan).
E-mail addresses: fcf728@163.com (C. Fan), swang2099@whu.edu.cn (S. Wang).
[1] Contributed equally.

https://doi.org/10.1016/j.preghy.2019.06.009
Received 31 January 2019; Received in revised form 28 June 2019; Accepted 28 June 2019
Available online 29 June 2019

and that they rarely contain multiple binding sites for the same miRNAs [7]. Thus, it seems unlikely that many circRNAs can function as miRNA sponges. In addition, several studies have indicated that some circRNAs, such as circMbl and circFOXO3 [8,9], can interact with different proteins to form specific circRNA binding proteins that subsequently influence modes of action of associated proteins. We were surprising to find that those two circRNAs target the protein encoded by their host genes. Moreover, the loop conformation protects circRNAs against RNA exonuclease, which allows them to maintain a stable expression level and makes them suitable diagnostic biomarkers for human diseases [10,11].

A few studies have reported the potential significance of circRNAs in the occurrence of PE [12–14]. Zhang's [15] groups first reported that the circ_101222 levels in blood corpuscles of patients with PE were significantly higher than those in corresponding healthy women. Qian's [16] and Hu's [14] groups discovered that circRNAs may contribute to the pathogenesis of PE by acting as miRNA sponges shortly afterwards. Unfortunately, most previous studies employed circRNA microarrays to detect circRNA expression. Obviously, compared with RNA-Seq, circRNA microarray technology has many limitations, and it is vulnerable to interference by the background signal and hybridization [17]. In this study, we applied RNA-Seq technology to identify DE-circRNAs in SPE placentae to provide a new avenue for mechanistic research of PE.

2. Materials and methods

2.1. Sample collection

All study patients were recruited from the Department of Obstetrics, Renmin Hospital of Wuhan University between June and October 2017. The patients, who had no previous history of high blood pressure, were diagnosed with SPE according to the following criteria: a systolic blood pressure (SBP) of 140–160 mm Hg or diastolic BP (DBP) levels of 90–110 mm Hg, measured at least two times with a 6 h interval after 20 weeks of gestation, along with new evidence of thrombocytopenia (< 100,000/mL), elevated liver enzymes, severe right-upper-quadrant pain that was resistant to medical treatment, pulmonary edema, cerebral and visual symptoms, and progressive renal failure (serum creatinine > 1.1 mg/dL) (Report of the American College of Obstetricians and Gynecologists' Task Force on Hypertension in Pregnancy, 2013). The inclusion criteria were singleton gestation, caesarean section, healthy pregnant women, and SPE patients. The exclusion criteria included multiple pregnancy, gestational diabetes mellitus, intrahepatic cholestasis of pregnancy, HELLP syndrome, pregnancies with chromosomal aberrations, foetal and placental structural abnormalities, and systemic chronic diseases. The diagnosis of intrauterine growth restriction (IUGR) was defined as predictive foetal weight < 5 percentile for gestational age [18]. The placenta samples were collected and dissected around the umbilical cord root at the time of the caesarean section and frozen in liquid nitrogen. Our project was reviewed and approved by the Ethics Committee of Renmin Hospital of Wuhan University, and all participants signed informed consent.

2.2. RNA extraction and qualification

Total RNA from human placentae was extracted using TRIzol reagent (Invitrogen, Life Technologies, USA) according to the manufacturer's protocol. The sequencing screening criteria for total RNA were as follows: OD260/OD280 = 1.8–2.2, 28S:18S ≥ 1.2, RIN ≥ 7.0, and total quality > 2 μg.

2.3. Library preparation and sequencing

First, ribosomal RNA was removed from the total RNA using the Ribo-Zero™ Gold kit. Next, RNA was fragmented into short segments (200–500 nt) by Fragmentation Buffer. The first strand of cDNA was synthesized by random Hexamers using the RNA fragment as a template. And then, the buffer, dNTPs, RNase H, and DNA Polymerase I were added into the mix to synthesize the second strand of cDNA. After purification, the end repairment, adding single base A and adding sequencing adapters of cDNA were successively finished. Finally, the target size fragments were purified by agarose gel electrophoresis, and the second strand of cDNA was digested with UNG enzyme and subjected to PCR amplification. An Illumina HiSeq™ 4000 system was used for sequencing.

Table 1
Demographic and clinical characteristics of the subjects.

Characteristics	SPE (n = 3)	NP (n = 3)	*P* value
Age at gestation (year)	33.00 ± 2.65	32.33 ± 4.04	0.823
Gestational age (day)	249.33 ± 2.08	251.33 ± 3.21	0.417
Gravidity	3.33 ± 0.58	2.33 ± 0.57	0.711
Parity	0.33 ± 0.57	1.00 ± 0.00	0.180
Pre-pregnancy BMI (kg/m^2)	25.40 ± 2.47	23.26 ± 3.35	0.423
BMI (kg/m^2)	29.92 ± 0.54	26.74 ± 3.21	0.166
Gestational weight gain (kg)	12.00 ± 7.00	9.00 ± 3.00	0.533
SBP (mmHg)	157.00 ± 22.11	115.33 ± 10.41	0.042*
DBP (mmHg)	95.33 ± 10.12	74.00 ± 10.58	0.065
Fetus birth weight (g)	2223.33 ± 323.32	3100.00 ± 522.02	0.069
IUGR rate (%)	1 (33.34%)	0	0.500
Apgar score	8.67 ± 0.58	9.67 ± 0.58	1.101

*P < 0.05.

2.4. CircRNA identification

CircRNAs were detected by CIRCexplore as previously reported [19]. First, we used the BWA-MEM algorithm to match the sequence to the reference genome, and the results were compared with SAM file scanning, searching for paired chiastic clipping, paired-end mapping loci, and GT-AG splicing signals. Finally, reads with only one junction site were remapped by a dynamic programming algorithm to ensure the reliability of circRNA identification. All sequencing procedures and analyses were performed by Annoroad Gene Technology Co., Ltd. (Beijing, China).

2.5. Characterization of circRNAs

Illumina HiSeq was applied in sample progression with an average of more than 120 million reads, and HiSAT2 was used for mapping them to the human reference genome (GRCh37/hg19). We used DEseq2 [20] to analyse the aberrant expression of circRNAs. Then, we identified DE-circRNAs between NP and SPE samples according to following criteria: $|\log_2(\text{fold changes})| \geq 1.5$ and p-values < 0.05. Finally, the allocation in chromosomes and the host genes of dysregulated circRNAs were also analysed.

2.6. Bioinformatics analysis

Gene Ontology (GO) analysis (http://www.geneontology.org) of the host genes of the DE-circRNAs was conducted. P-values < 0.05 were considered significant. Pathway analysis was conducted on the Kyoto Encyclopedia of Genes and Genomes (KEGG) database to determine host genes in diverse biological processes. The significance of pathways was negatively correlated with p-values ($p < 0.05$). Gene Set Enrichment Analysis (GSEA) was established based on the host gene expression data of the circRNAs to further confirm the results of GO and KEGG analysis. The network visualization and analysis tool Cytoscape_V2_8_3 was used to identify putative target genes for the predicted miRNA sponges.

Table 2
Primers of selected DE-circRNAs for qRT-PCR.

circRNA	F-primer	R-primer	Predict length of product (bp)
hsa_circ_0007611	CTGGGGTGGTAAAACTTGGAGA	CTAATGTATTATAGCCCATATCCGG	193
hsa_circ_0011460	TTTTCTCTCTACAAGCCATTCCC	CCTCCAACTTCCTTGCTTCATCT	164
hsa_circ_0002888	CACCTTGGTTGTGGCTGACTC	CACCATTTCAGGCAAAGACCA	238
hsa_circ_0007445	AACCTGTCAAAGTCCAGAGCAT	GGATAGTGAGGGACTTGTTGCT	245
hsa_circ_0017068	GAAGTTTTAGAGGAATGGCAGTCTC	TTGAGCATTAGGTTCGGGGTG	207
hsa_circ_0012737	TGGAGAACCTATCAAGATGCGA	TGAGACTGACAAACAGAAGCCAC	226
H-ACTIN	CACCCAGCACAATGAAGATCAAGAT	CCAGTTTTTAAATCCTGAGTCAAGC	317

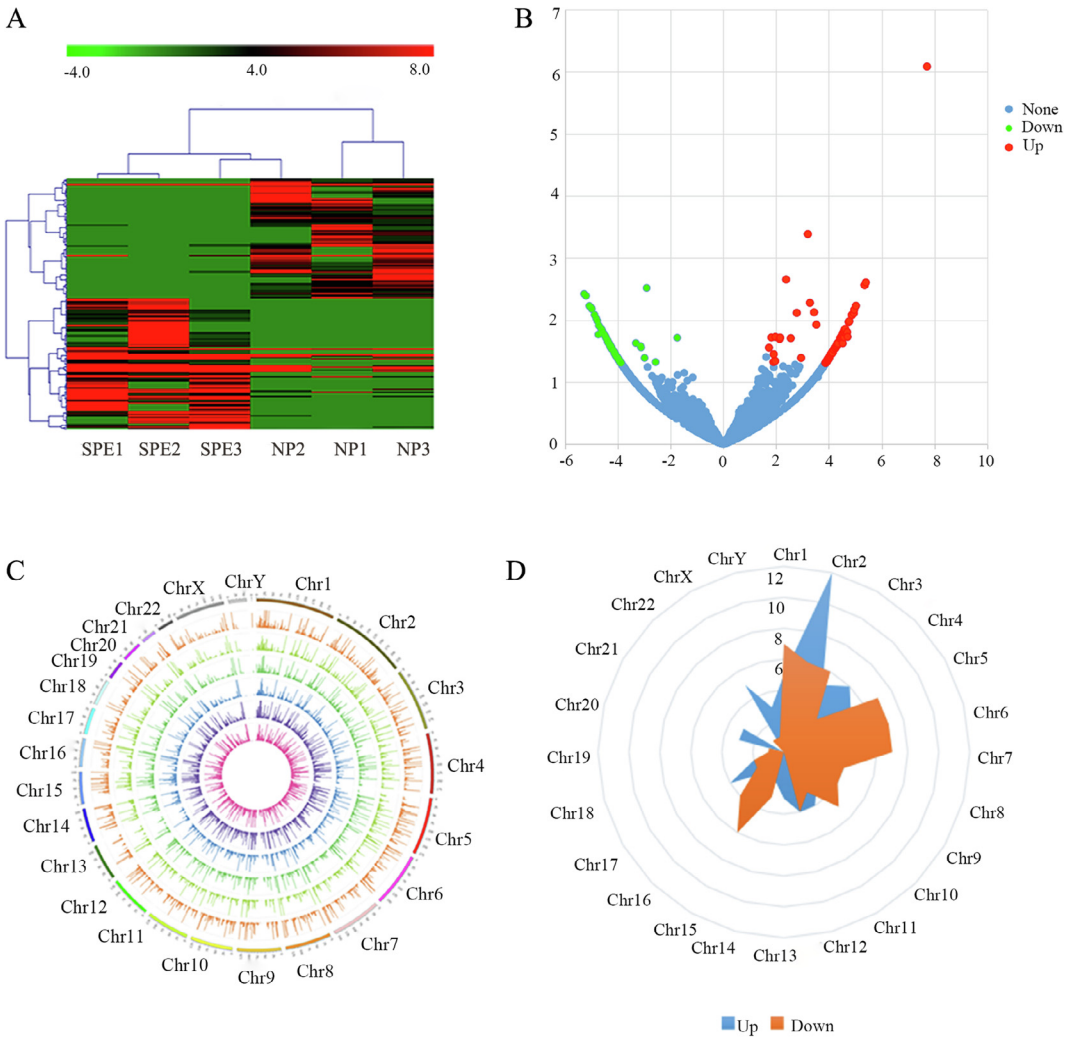

Fig. 1. Expression profiles of circRNAs between SPE and normotensive groups. (A) Hierarchical cluster analysis was based on the expression values of all dysregulated circRNAs detected by RNA-Seq. The red colour indicates positive relative expression, and the green colour denotes negative relative expression, $n = 3$ each group. One column indicates one sample, and one row indicates a transcript. (B) DE-circRNAs in SPE samples compared with NP samples. FC, fold change. (C) The circus plot presents the distribution of abundance of all circRNAs on different chromosomes. The expression value (FPKM) of all circRNA transcripts is presented based on their locations in the human reference genome. (D) Overview of the distribution of differently expressed circRNAs is based on the number of circRNAs. Blue colour indicates upregulation, and pink colour represents downregulation. (For interpretation of the references to colour in this figure legend, the reader is referred to the web version of this article.)

2.7. qRT-PCR

qRT-PCR was performed with SYBR ®Premix Ex Taq™ II (TaKaRa, Japan) according to the manufacturer's protocol. β-actin was used as an internal RNA control, and the expression levels of the target circRNAs were calculated through the 2-ΔΔCt method. The primer sequences are shown in Table 2.

2.8. Cell culture

Human first trimester trophoblast cell line (HTR-8/SVneo) cells were purchased from the American Type Culture Collection (ATCC) and cultured in RPMI 1640 (Gibco, USA) with 10% FBS (Gibco, USA) and 1% penicillin/streptomycin at 37°C and 5% CO2 for further RIP assays.

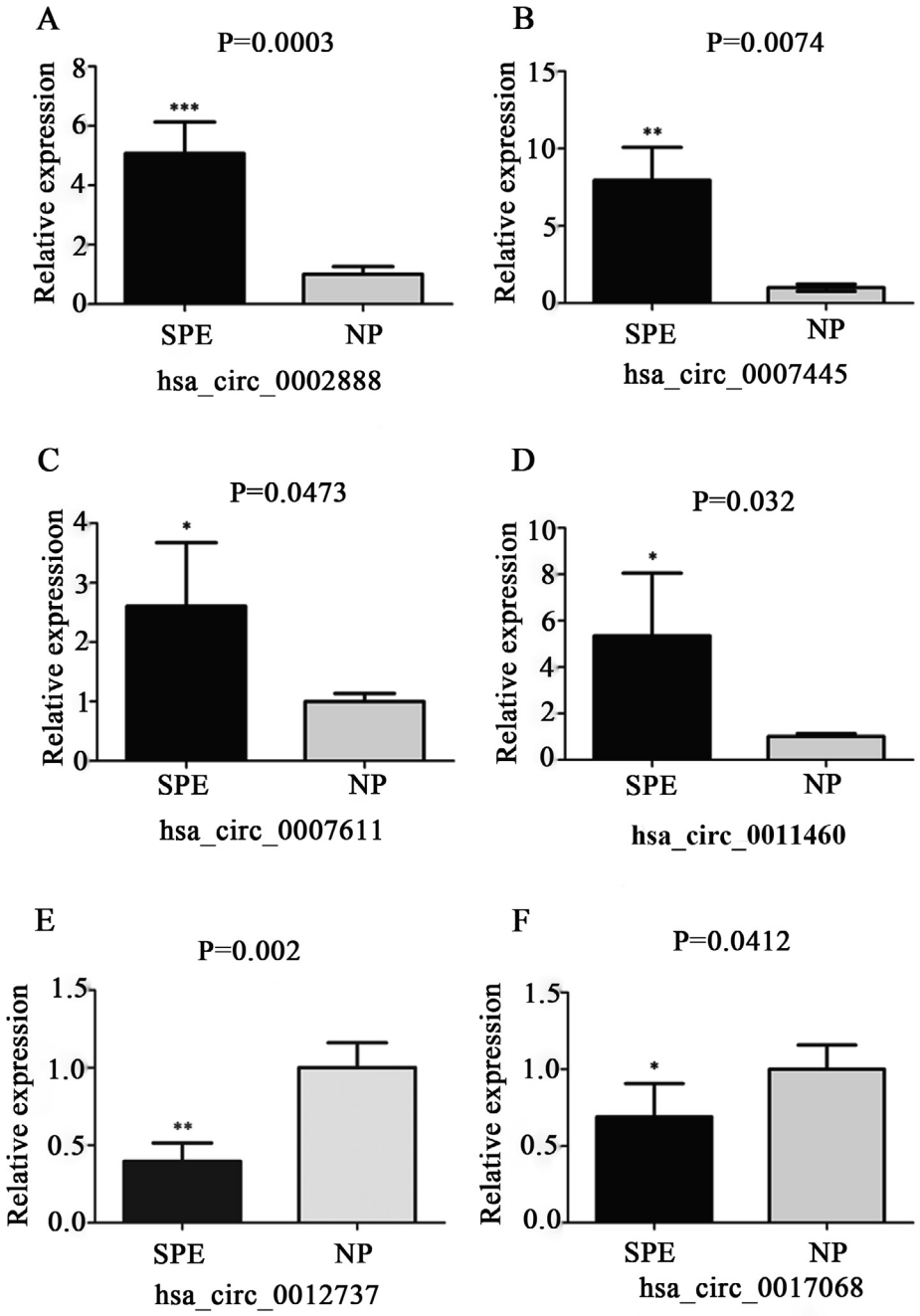

Fig. 2. qRT-PCR confirmed the RNA-Seq data of the six circRNAs (four upregulated and two downregulated) using divergent primers. (A) hsa_circ_0002888 (B) hsa_circ_0007445 (C) hsa_circ_0007611 (D) hsa_circ_0011460 (E) hsa_circ_0012737 (F) hsa_circ_0017068. Values are the mean ± SD (n = 3 per group). qRT-PCR analysis was conducted in triplicate. *p < 0.05 compared with sham (Student's *t*-test). SPE indicates severe preeclampsia, NP indicates normal aged pregnancy.

2.9. RNA immunoprecipitation

RIP experiments were performed using a Magna RIP RNA Binding Protein Immunoprecipitation Kit (Millipore, Bedford, MA, USA). The PGT-RIP assay was conducted in HTR-8/SVneo cells. Approximately 1×10^7 cells were pelleted and resuspended in an equal volume of RIP lysis buffer (approximately 100 μl) containing protease and RNase inhibitors. Cell lysates (100 μl) were incubated with 5 μg control rabbit IgG- or anti-PGT antibody (Abcam ab150788)-coated beads with rotation at 4 °C overnight. After treatment with proteinase K, the immunoprecipitated RNAs were extracted using the RNeasy MinElute Cleanup Kit (QIAGEN) and reverse transcribed using Prime-Script RT Master Mix (TaKaRa). The level of hsa_circ_0011460 was detected by qRT-PCR.

2.10. Immunohistochemistry

Collected specimens were subjected to immunohistochemistry analysis using the Enovision Detection Kit/DAB (GK500705, DAKO A/S, Glostrup, Denmark) according to the manufacturer's protocol with the indicated antibody: anti-PGT antibody (Abcam ab150788). The images were acquired with a Leica DM25000B microscope (Leica, Germany).

2.11. Western blotting

Cell lysates/placenta protein were extracted using enhanced RIPA

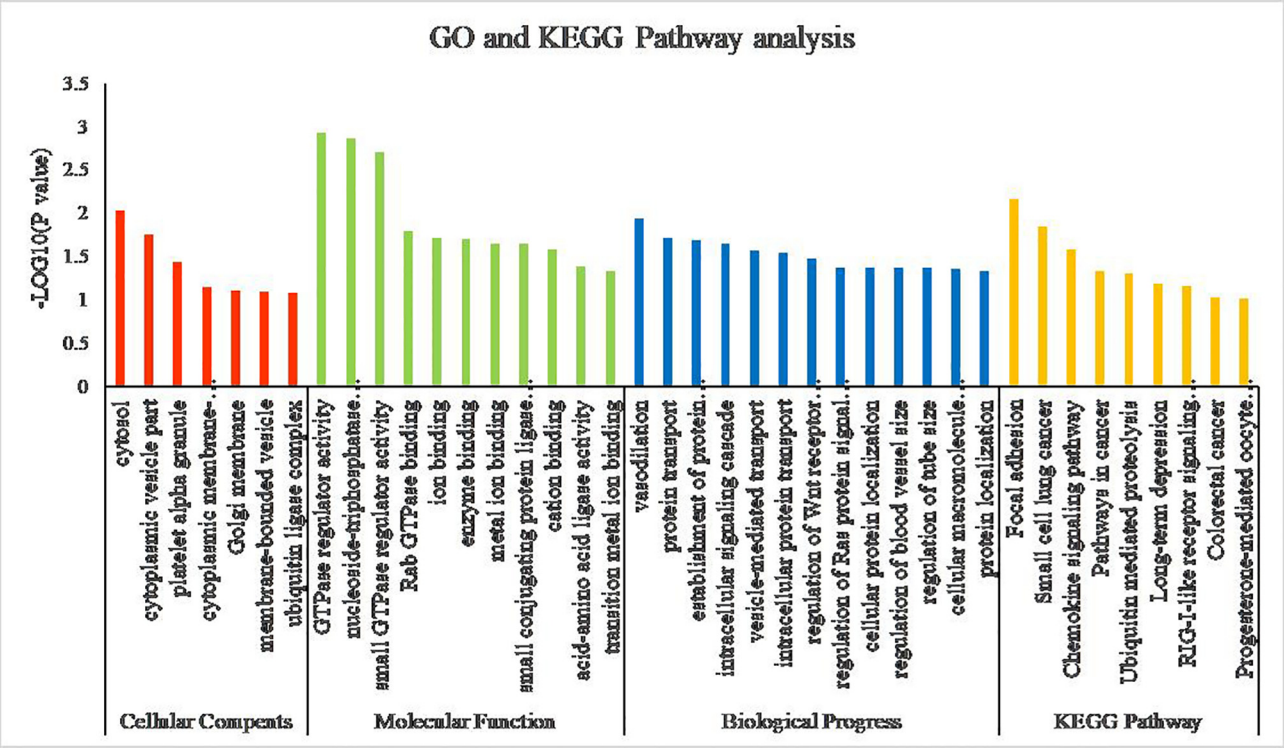

Fig. 3. Gene Ontology analysis and Kyoto Encyclopedia of Genes and Genomes pathway analysis for dysregulated circRNA gene symbols. Red columns indicate enriched biological process of dysregulated circRNA gene symbols; green columns indicate enriched molecular function of dysregulated circRNA gene symbols; blue columns indicate cellular component of dysregulated circRNA gene symbols and yellow columns indicate enriched KEGG pathways of dysregulated circRNA gene symbols.

Lysis Buffer (Beyotime) containing a 1% dilution of PMSF (Beyotime). Protein concentrations were determined using a microplate reader (Bio-TEK, USA) with the enhanced BCA Protein Assay kit (Beyotime). Equal amounts of protein in each lane were separated by 8–10% SDS-PAGE and transferred to a 0.45 μm PVDF membrane (Millipore, Billerica, MA, USA). After blocking the membrane in 5% nonfat milk, the membrane was incubated with primary antibodies at 4 °C overnight, followed by incubation with labelled secondary antibody at room temperature for 1 h, washing, and addition of Immobilon Western Chemiluminescent HRP Substrate (Millipore, USA). Imaging was performed using a GelDoc XR System (Bio-Rad, USA).

2.12. Statistical analysis

All experiments were conducted at least in triplicate, and the results are expressed as the mean ± standard error of the mean (SEM). An independent sample *t* test was performed using SPSS 21.0 to detect significant differences in the measured variables between the two groups. A P-value < 0.05 was considered statistically significant.

3. Results

3.1. Demographic and clinical characteristics of the participants

The demographic and clinical information of each participant in this study is summarized in Table 1. Cases for RNA-Seq were artificially matched for maternal age, gestational weeks and body mass index (BMI).

3.2. CircRNA profiles in human placentae

First, we characterized the circRNA transcripts using RNA-Seq analysis of ribosomal RNA-depleted total RNA from three NP and three SPE placentae. A computational pipeline based on the anchor alignment of unmapped reads was used to identify circRNAs without relying on gene annotations. In total, 18,631 distinct circRNA candidates, containing at least two unique backspliced reads, were found in these tissues. Among them, 180 circRNAs were screened out as DE-circRNAs, including 94 upregulated and 86 downregulated circRNAs. The volcano plot and the hierarchical cluster are presented to visualize the results (Fig. 1A, B). The distribution of DE-circRNAs among chromosomes is presented in Fig. 1D. Obviously, most upregulated circRNAs were distributed on chromosome 2, while the majority of downregulated circRNAs were centralized on chromosomes 5, 6 and 15. Furthermore, after mapping all detected circRNA candidates to the human reference genome, a circus plot was generated to show the landscape of circRNA candidate abundance distribution among different chromosomes on the basis of fragments per kilobase of transcript per million (FPKM) (Fig. 1C). Most circRNA candidates were centralized on chromosomes 1–7 and X. All these results indicate that the expression profiles of circRNAs in the placenta were different between SPE and NP.

3.3. Validation of circRNA expression

We selected 7 of the top 10 distinctly up- or downregulated circRNAs for further validation by qRT-PCR. One-generation sequencing of qRT-PCR products was conducted to detect the junction reads of selected circRNAs. Among them, the qRT-PCR results of 6 DE-circRNAs (hsa_circ_0002888, hsa_circ_0007445, hsa_circ_0007611, hsa_circ_0011460, hsa_circ_0012737, hsa_circ_0017068) were consistent with the RNA-Seq data (Fig. 2), while one circRNA-hsa_circ_0017068 presented the opposite expression trend between the RNA-Seq data and qRT-PCR results.

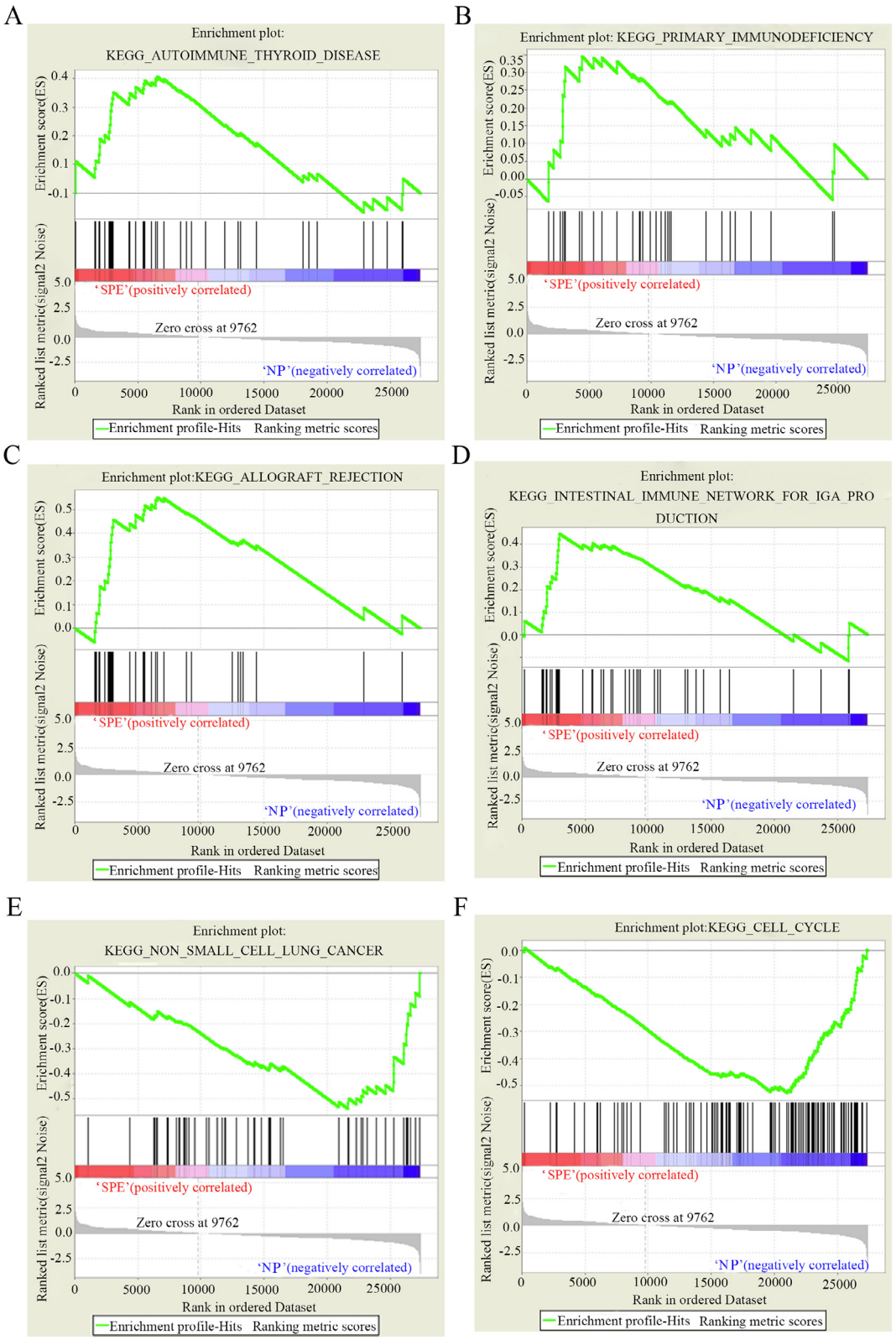

Fig. 4. Gene set enrichment analysis (GSEA) with a high enrichment score for gene sets. (A) Autoimmune thyroid disease (B) primary immunodeficiency (C) allograft rejection (D) intestinal immune network for IGA production (E) non-small cell lung cancer (F) cell cycle.

3.4. GO and KEGG pathway analyses

GO analysis (Fig. 3), consisting of biological process, cellular component, and molecular function, revealed that the majority of DE-circRNAs are involved in vasodilation, regulation of blood vessel size, protein transport and localization. To investigate the role of circRNAs in gene regulation, KEGG pathway enrichment analysis was conducted based on the parent genes of DE-circRNAs. The top ranked pathways include pathways in cancer, chemokine signalling pathway and focal adhesion (Fig. 3).

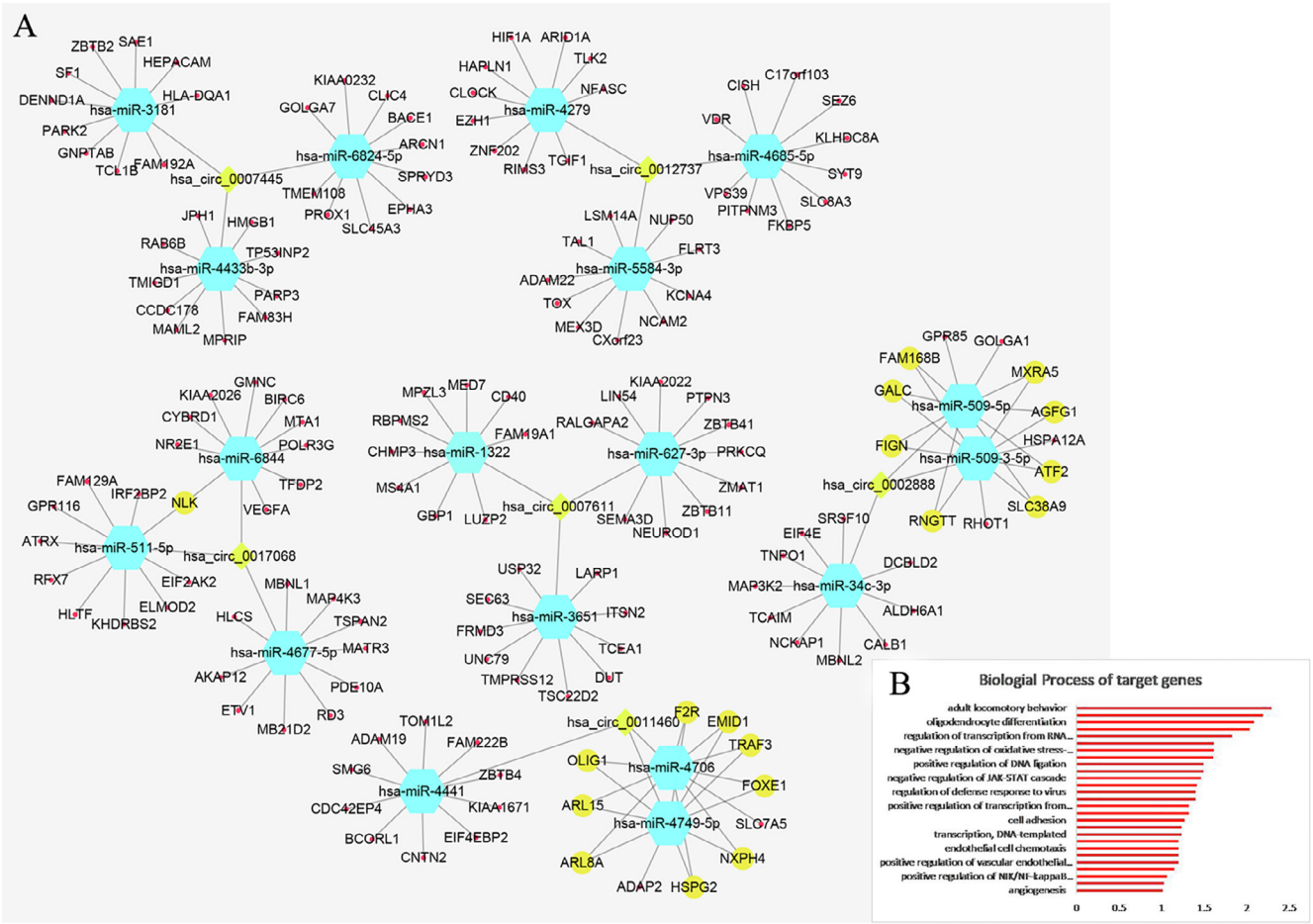

Fig. 5. CeRNA network in SPE. The ceRNA network was based on circRNA/miRNA and miRNA/mRNA interactions. In this network, the edges represent sequence matching, and circRNAs connect the expression of mRNAs through miRNAs. The ceRNA network of hsa_circ_0007611, hsa_circ_0011460, hsa_circ_0002888, hsa_circ_0007445, hsa_circ_0017068 and hsa_circ_0012737. Diamond nodes (light green) represent circRNAs, hexagon nodes (light blue) represent miRNAs, and round nodes (orange) represent correlated mRNAs. The size of the node indicates the number of interactions. (For interpretation of the references to colour in this figure legend, the reader is referred to the web version of this article.)

3.5. Gene set enrichment analysis (GSEA)

GSEA was conducted to validate whether DE-circRNAs are associated with PE-related pathways. Significantly enriched gene sets were positively related to the pathways of autoimmune thyroid disease (Fig. 4A), primary immunodeficiency (Fig. 4B), allograft rejection (Fig. 4C), and intestinal immune network for IGA production (Fig. 4D) and negatively related to the pathways of cell cycle and non-small cell lung cancer (Fig. 4E), which are related to oxidative stress activation, inflammatory reaction and cell survival, death, differentiation, proliferation, and neuroinflammation (Fig. 4F).

3.6. Construction of the ceRNA network

To explore the miRNA sponge potential of validated circRNAs, the target miRNAs of four upregulated circRNAs (hsa_circ_0007611, hsa_circ_0011460, hsa_circ_0002888, and hsa_circ_0007445) and two downregulated circRNAs (hsa_circ_0017068 and hsa_circ_0012737) as well as the downstream genes of these miRNAs were predicted by using Cytoscape_V2_8_3. The top 3 predicted miRNAs and the top 10 mRNAs were enrolled. Finally, a global ceRNA network was constructed and was presented in Fig. 5A. Further biological processes of those target genes were analysed (Fig. 5B). Angiogenesis, response to hypoxia, inflammatory response and VEGFR signal pathway were all involved and have been reported to participate in the occurrence of PE.

3.7. Validation of PGT expression

Interestingly, according to GO analysis, protein transport and localization were considerably enriched. Combined with the mRNA expression profile of the placentae (Fig. 6A, B), we unexpectedly found that the solute carrier organic anion transporter family member 2A1-PGT, the host gene of hsa_circ_0011460, was also significantly increased in SPE placentae. We finally chose hsa_circ_0011460 as our target circRNA. Online bioinformatic tools (RNA-Protein Interaction Prediction, RPIP) predicted that hsa_circ_0011460 may target the PGT protein directly. Thus, we validated the higher mRNA expression of PGT in human placentae of SPE than in NP (n = 15, n = 15) by qRT-PCR (Fig. 6C) and further confirmed its protein expression by Western blotting and immunohistochemistry (Fig. 6D–G). Furthermore, we found that PGT was mainly located in syncytiotrophoblasts and cytotrophoblasts by immunohistochemistry (Fig. 6 D, E).

3.8. hsa_circ_0011460 directly interacts with PGT

To further confirm the direct interaction of hsa_circ_0011460 and PGT, RIP was employed. RIP in HTR-8/SVneo cells showed that the level of endogenous hsa_circ_0011460 pulled down by PGT antibody was significantly higher than the control using IgG antibody (Fig. 7). All these data suggest that hsa_circ_0011460 targets PGT directly.

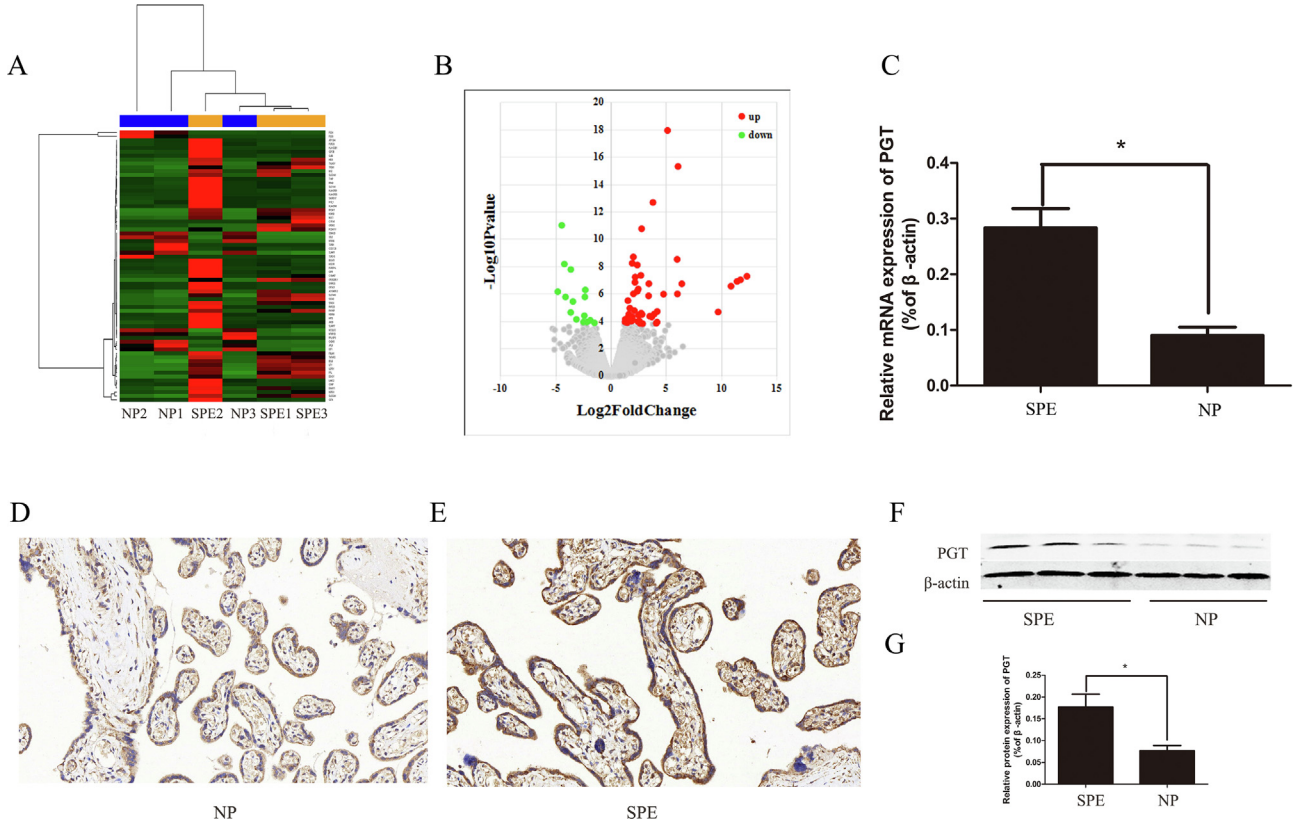

Fig. 6. The expression of PGT in human placentae. (A) Hierarchical cluster analysis of dysregulated mRNAs detected by RNA-Seq. The red colour indicates positive relative expression, and the green colour denotes negative relative expression, n = 3 each group. One column indicates one sample, and one row indicates a transcript. (B) DE-mRNAs in SPE samples compared with normal samples. FC, fold change; (C) mRNA expression of PGT in the placenta of matched NP and SPE by qRT-PCR, n = 15 each group. (D), (E) Immunohistochemistry of PGT in the placentae of matched normal pregnancy and SPE; (F), (G) Western blotting of PGT in placentae of matched SPE and NP.

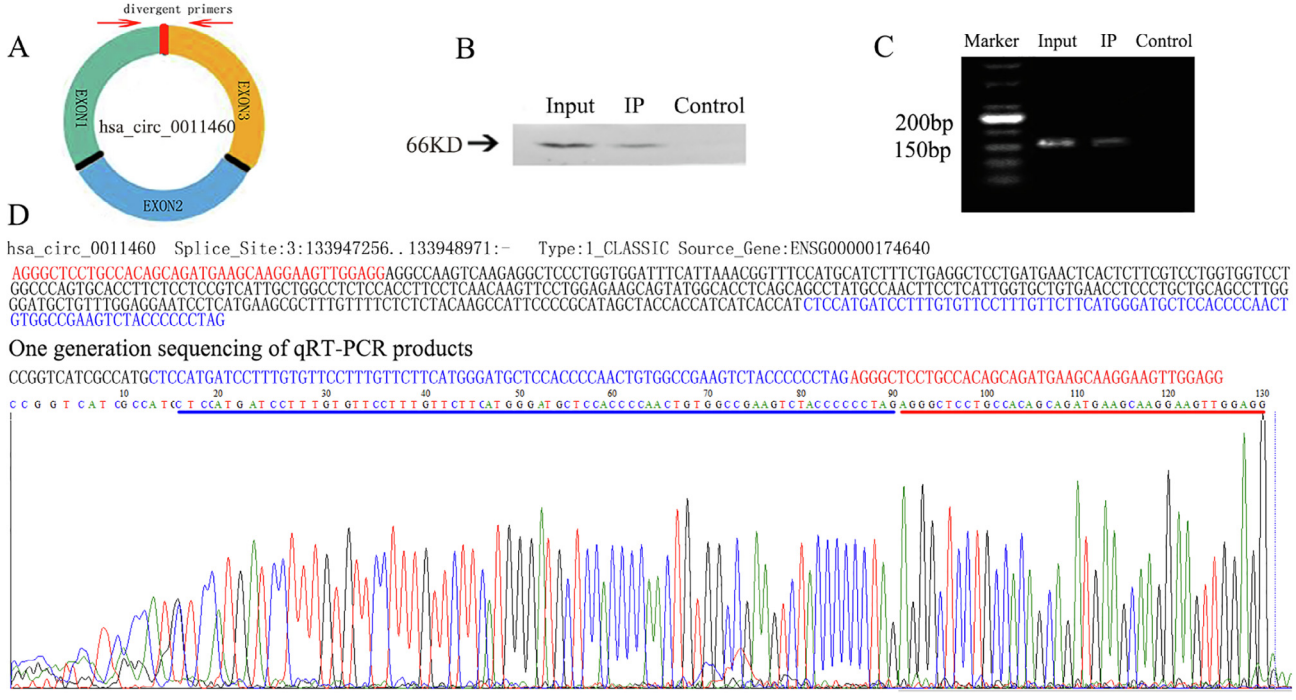

Fig. 7. hsa_circ_0011460 directly interacts with PGT. (A) The ring frame of hsa_circ_0011460; (B) Western blotting of protein samples obtained from immunoprecipitation. The input and target lanes showed obvious bands at a position of approximately 66 kDa, and the negative control sample had no band. (C) The RNA samples obtained from immunoprecipitation were used as a template, and qRT-PCR amplification was carried out using a specific RIP primer. The PCR product of hsa_circ_0011460 (hsa_circ_0011460 was 164 bp) was analysed by gel electrophoresis. (D) Basic information about hsa_circ_0011460 and one generation sequencing result of qRT-PCR products.

4. Discussion

In this study, we systematically profiled DE-circRNAs in the placentae of SPE patients by integrating RNA-Seq data in human SPE and NP placentae. A total of 18,631 circRNAs were detected. Among them, 180 circRNAs were differentially expressed in SPE placentae, including 94 upregulated and 86 downregulated circRNAs. The majority of detected circRNAs have not been annotated previously. Consistent with other groups' work, our study indicated that the expression profiles of circRNA in placentae were apparently different between SPE and NP.

Several bioinformatics tools were applied to integrate the RNA-Seq data, and a global ceRNA network was depicted. As shown in Fig. 2, many DE-circRNAs were enriched in vasodilation, regulation of blood vessel size, protein transport and localization. As delineated in the two-stage theory of PE, the pathogenesis of PE is rooted in early pregnancy, while clinical symptoms manifested until late pregnancy [21]. In the second two trimesters of pregnancy, the placenta requires increasing access to the maternal blood supply, which is created by extensive remodelling of maternal spiral arteries [22]. This finding indirectly suggests that vasodilation and regulation of blood vessel size may be involved in the onset of PE. In addition, clinical studies [23,24] reported that maternal endothelial function and aberrant concentrations of the endogenous inhibitor of endothelial nitric oxide synthase (ADMA) were associated with PE. Huang et al. [25] reported that PE is associated with impaired maternal-foetal nutrient transfer, and the amino acid transporters SLC7A7 and SLC38A5 showed marked differences between controls and PE. However, the crucial transport mechanisms underlying PE have not been fully elucidated. Based on the mRNA profiles and validation results by qRT-PCR, we ultimately chose hsa_circ_0011460 as our target circRNA, whose parent gene is PGT, which encodes a prostaglandin transporter that is a member of the 12-membrane-spanning superfamily of transporters and is involved in mediating the uptake and clearance of prostaglandins in numerous tissues, especially prostaglandin E2 (PGE2) [26]. PGE2 was shown to promote the migration of HTR-8/SVneo cells and is associated with decidualization [27,28].

The genomic structure shows that hsa_circ_0011460, a classical circular RNA, consists of three exons (434 bp) from the PGT gene locus (Fig. 7a). Considering that only a few circRNAs can function as miRNA sponges, we focused on studying circRNA function by sequestering proteins. Online bioinformatics tools unexpectedly predicted that hsa_circ_0011460 may target the protein PGT encoded by its parent gene. A previous study speculated that there is a feedback loop between MBL and circMbl production. When the protein is in excess, it decreases the production of its own mRNA by promoting circMbl production. This circRNA could then sponge the excess MBL protein by binding to it [8]. Such a model of action of circRNA was also observed in the highly expressed circFOXO3 in the mammalian heart [9]. Consistent with that of hsa_circ_0011460, the level of PGT protein was significantly higher in the placentae of SPE compared with NP in further verification studies. Immunohistochemistry of PGT showed that PGT protein was mainly distributed in syncytiotrophoblasts and cytotrophoblasts. Finally, RIP assays of HTR-8/SVneo cells showed that hsa_circ_0011460 directly interacts with PGT.

Based on these results, we speculated that hsa_circ_0011460 may participate in the occurrence and development of SPE by anchoring the protein of PGT. This finding provides a new avenue for research on PE, and this molecule may be a biomarker of the early diagnosis of SPE that has been studied in our subsequent work. The detailed molecular mechanism needs to be further studied.

Ethics approval and consent to participate

All patients signed informed consent, and the study was approved by the Wuhan University Ethics Committee.

Consent for publication

The text and any pictures published in the article will be freely available on the internet and may be seen by the general public. The pictures and text may also appear on other websites or in print and may be translated into other languages or used for commercial purposes.

Authors' contributions

Na Deng and Jinfa Huang performed the data analysis and wrote the draft; Di Lei and Zhuanhong Yang collected samples; Di lei and Cuifang Fan and Suqing Wang designed the study and helped draft the manuscript. All authors read and approved the final manuscript.

Funding

No funding support for this article.

Declaration of Competing Interest

The authors declared that they have no conflicts of interest.

Acknowledgements

The authors thank all the members for their valuable assistance and comments on the manuscript.

Appendix A. Supplementary data

Supplementary data to this article can be found online at https://doi.org/10.1016/j.preghy.2019.06.009.

References

[1] B. Mol, C.T. Roberts, S. Thangaratinam, L.A. Magee, C. de Groot, G.J. Hofmeyr, Pre-eclampsia, Lancet 387 (2016) 999–1011.
[2] B. Capel, A. Swain, S. Nicolis, A. Hacker, M. Walter, P. Koopman, P. Goodfellow, R. Lovell-Badge, Circular transcripts of the testis-determining gene Sry in adult mouse testis, Cell 73 (1993) 1019–1030.
[3] S.J. Conn, K.A. Pillman, J. Toubia, V.M. Conn, M. Salmanidis, C.A. Phillips, S. Roslan, A.W. Schreiber, P.A. Gregory, G.J. Goodall, The RNA binding protein quaking regulates formation of circRNAs, Cell 160 (2015) 1125–1134.
[4] S. Memczak, M. Jens, A. Elefsinioti, F. Torti, J. Krueger, A. Rybak, L. Maier, S.D. Mackowiak, L.H. Gregersen, M. Munschauer, A. Loewer, U. Ziebold, M. Landthaler, C. Kocks, F. le Noble, N. Rajewsky, Circular RNAs are a large class of animal RNAs with regulatory potency, Nature 495 (2013) 333–338.
[5] X. Li, L. Yang, L.L. Chen, The biogenesis, functions, and challenges of circular RNAs, Mol. Cell 71 (2018) 428–442.
[6] T.B. Hansen, T.I. Jensen, B.H. Clausen, J.B. Bramsen, B. Finsen, C.K. Damgaard, J. Kjems, Natural RNA circles function as efficient microRNA sponges, Nature 495 (2013) 384–388.
[7] J.U. Guo, V. Agarwal, H. Guo, D.P. Bartel, Expanded identification and characterization of mammalian circular RNAs, Genome Biol. 15 (2014) 409.
[8] R. Ashwal-Fluss, M. Meyer, N.R. Pamudurti, A. Ivanov, O. Bartok, M. Hanan, N. Evantal, S. Memczak, N. Rajewsky, S. Kadener, circRNA biogenesis competes with pre-mRNA splicing, Mol. Cell 56 (2014) 55–66.
[9] W. du Ww, Y. Yang, Z.K. Chen, F.S. Wu, Z. Foster, X. Yang, B.B. Li, Yang, Foxo3 circular RNA promotes cardiac senescence by modulating multiple factors associated with stress and senescence responses, Eur. Heart J. 38 (2017) 1402–1412.
[10] S. Memczak, P. Papavasileiou, O. Peters, N. Rajewsky, Identification and characterization of circular RNAs as a new class of putative biomarkers in human blood, PLoS One 10 (2015) e0141214.
[11] Y. Li, Q. Zheng, C. Bao, S. Li, W. Guo, J. Zhao, D. Chen, J. Gu, X. He, S. Huang, Circular RNA is enriched and stable in exosomes: a promising biomarker for cancer diagnosis, Cell. Res. 25 (2015) 981–984.
[12] W. Zhou, H. Wang, X. Wu, W. Long, F. Zheng, J. Kong, B. Yu, The profile analysis of circular RNAs in human placenta of preeclampsia, Exp. Biol. Med. (Maywood) 243 (2018) 1109–1117.
[13] M. Jiang, G.E. Lash, X. Zhao, Y. Long, C. Guo, H. Yang, CircRNA-0004904, CircRNA-0001855, and PAPP-A: potential novel biomarkers for the prediction of pre-eclampsia, Cell. Physiol. Biochem. 46 (2018) 2576–2586.
[14] X. Hu, J. Ao, X. Li, H. Zhang, J. Wu, W. Cheng, Competing endogenous RNA expression profiling in pre-eclampsia identifies hsa_circ_0036877 as a potential novel blood biomarker for early pre-eclampsia, Clin. Epigenet. 10 (2018) 48.
[15] Y.G. Zhang, H.L. Yang, Y. Long, W.L. Li, Circular RNA in blood corpuscles combined

with plasma protein factor for early prediction of pre-eclampsia, BJOG 123 (2016) 2113–2118.
[16] Y. Qian, Y. Lu, C. Rui, Y. Qian, M. Cai, R. Jia, Potential significance of circular RNA in human placental tissue for patients with preeclampsia, Cell. Physiol. Biochem. 39 (2016) 1380–1390.
[17] S. Zhao, W.P. Fung-Leung, A. Bittner, K. Ngo, X. Liu, Comparison of RNA-Seq and microarray in transcriptome profiling of activated T cells, PLoS One 9 (2014) e78644.
[18] K. Zhang-Rutledge, L.M. Mack, J.M. Mastrobattista, M. Gandhi, Significance and outcomes of fetal growth restriction below the 5th percentile compared to the 5th to 10th percentiles on midgestation growth ultrasonography, J. Ultrasound Med. 37 (2018) 2243–2249.
[19] X.O. Zhang, H.B. Wang, Y. Zhang, X. Lu, L.L. Chen, L. Yang, Complementary sequence-mediated exon circularization, Cell 159 (2014) 134–147.
[20] M.I. Love, W. Huber, S. Anders, Moderated estimation of fold change and dispersion for RNA-seq data with DESeq2, Genome Biol. 15 (2014) 550.
[21] B. Alasztics, Z. Kukor, Z. Panczel, S. Valent, The pathophysiology of preeclampsia in view of the two-stage model, Orv. Hetil. 153 (2012) 1167–1176.
[22] C.W. Redman, I.L. Sargent, Latest advances in understanding preeclampsia, Science 308 (2005) 1592–1594.
[23] M.D. Savvidou, A.D. Hingorani, D. Tsikas, J.C. Frolich, P. Vallance, K.H. Nicolaides, Endothelial dysfunction and raised plasma concentrations of asymmetric dimethylarginine in pregnant women who subsequently develop pre-eclampsia, Lancet 361 (2003) 1511–1517.
[24] P.M. Sarrel, D.C. Lindsay, P.A. Poole-Wilson, P. Collins, Hypothesis: inhibition of endothelium-derived relaxing factor by haemoglobin in the pathogenesis of pre-eclampsia, Lancet 336 (1990) 1030–1032.
[25] X. Huang, P. Anderle, L. Hostettler, M.U. Baumann, D.V. Surbek, E.C. Ontsouka, C. Albrecht, Identification of placental nutrient transporters associated with intrauterine growth restriction and pre-eclampsia, BMC Genom. 19 (2018) 173.
[26] T. Nakanishi, I. Tamai, Roles of organic anion transporting polypeptide 2A1 (OATP2A1/SLCO2A1) in regulating the pathophysiological actions of prostaglandins, AAPS J. 20 (2017) 13.
[27] H. Horita, E. Kuroda, T. Hachisuga, M. Kashimura, U. Yamashita, Induction of prostaglandin E2 production by leukemia inhibitory factor promotes migration of first trimester extravillous trophoblast cell line, HTR-8/SVneo, Hum. Reprod. 22 (2007) 1801–1809.
[28] J. Kang, P. Chapdelaine, P.Y. Laberge, M.A. Fortier, Functional characterization of prostaglandin transporter and terminal prostaglandin synthases during decidualization of human endometrial stromal cells, Hum. Reprod. 21 (2006) 592–599.